Desalination and Water Treatment
www.deswater.com
doi: 10.5004/dwt.2020.25878

195 (2020) 177–185
August

Experimental design and RSM modeling of tetracycline photocatalytic degradation using rGO/ZnO/Cu

Maedeh Asgharian[a], Mohsen Mehdipourghazi[a,*], Behnam Khoshandam[a], Narjes Keramati[b]

[a]*Faculty of Chemical, Petroleum, and Gas Engineering, Semnan University, Semnan 35131–19111, Iran, Tel. +98 2331533922; Fax: +98 2333654120; emails: mohsenmehdipour@semnan.ac.ir (M. Mehdipourghazi), Maedeh.asgharian@gmail.com (M. Asgharian), b.khoshandam@semnan.ac.ir (B. Khoshandam)*
[b]*Faculty of Nanotechnology, Semnan University, Semnan, 35131–19111, Iran, email: narjeskeramati@semnan.ac.ir (N. Keramati)*

Received 25 July 2019; Accepted 23 March 2020

ABSTRACT

Tetracycline (TC) photodegradation using rGO/ZnO/Cu nano-powder was investigated under visible irradiation. The effect of operating conditions such as pH, photocatalyst concentration, and initial concentration of pollutant on reaction rate constant and total organic carbon (TOC) removal was studied. Complete removal of 40mg/L tetracycline concentrations was achieved at pH 8 and 1 g/L rGO/ZnO/Cu. The best model fitted to the experimental data was pseudo-second-order, with maximum and minimum kinetic rate constants of TC elimination estimated at 1 g/L (0.007280 L/min/mg) and photolysis (0.000018 L/min/mg), respectively. The TC and TOC removal percentages reached 100% and 91.2% after 180 and 300 min, respectively.

Keywords: ZnO/Cu; rGO; Tetracycline; Photodegradation; RSM

1. Introduction

Antibiotics are utilized to treat or prevent human and animal infections in modern medicine. One of the most commonly used antibiotics is tetracycline (TC) which is a bacteriostatic agent used to treat gram-positive and gram-negative bacteria, mycoplasma, and fungi [1]. As a result of its wide consumption (thousands of tons annually) and poor absorption in human and animal bodies, traces of TC, and their metabolites have been detected in many different environments [2]. TC has been found in very low concentration (μg/L or ng/L) in treated waters and higher levels (100–500 mg/L) in effluents of hospital and pharmaceutical manufacturing wastewaters [3,4]. It is considered a contaminant because of long persistence (slow degradation) in nature, inducing antibiotic-resistance in microorganisms, acute, and chronic activity in ecosystems and genetic exchanges [5].

Thus far, various chemical, physical, and biological methods have been used for TC absorption or degradation [6–12]. According to previous studies, some advanced oxidation processes are low cost and high-efficiency strategies [2]. Photocatalysts based on semiconductor metals like ZnO operate in ambient conditions and have few limitations. ZnO is activated in the UV region [13], but when corrected by a transient metal like Cu shifts to the visible range [14–16]. Reduced graphene oxide (rGO) acts as an electron sink diminishing electron–hole recombination, and enhancing the effectiveness of ZnO by its high surface area and changing electrical charge of the surface leading to reduced ZnO agglomeration [17–20]. It has been reported that ZnO activated with copper and rGO has higher photocatalytic activity and other improved properties [21].

* Corresponding author.

1944-3994/1944-3986 © 2020 Desalination Publications. All rights reserved.

The chain of photocatalytic reaction is facilitated by derived semiconductors, which have better performance by improving method procedure and/or material properties [22–24]. The reaction starts with adsorbing photons on the surface of the semiconductor. Photons activate electrons with an equal or higher energy to the bandgap and transfer valance band electrons (e^-) to the conduction band. The lack of electrons in the valance band generates holes (h^+) and the first reaction of the series takes place (reaction (1)). Then other molecules like H_2O and trapped OH^- on the catalyst surface get involved and produce hydroxyl radicals (reactions (2) and (3)). At the same time, promoted electrons attack the O_2 molecules and create superoxide ions ($^\bullet O_2$), followed by the production of hydrogen peroxide (H_2O_2) and hydroxyl ions (reactions (4) and (5)). Conduction band electrons react with H_2O_2 molecules and generate more OH^- and $OH^\bullet$ (reaction (6)). Photocatalytic reaction needs enough $OH^\bullet$ as a powerful oxidant and the h^+ as an electron-absorbing organic matter (OM) and ameliorative degradation reaction (reaction (7) and (8)) [22–24].

$$\text{Semiconductor} + h\nu \rightarrow e^- + h^+ \quad (1)$$

$$h^+ + H_2O \rightarrow H^+ + OH^\bullet \quad (2)$$

$$h^+ + OH^- \rightarrow OH^\bullet \quad (3)$$

$$e^- + O_2 \rightarrow O_2^\bullet \quad (4)$$

$$O_2^{\bullet -} + H_2O + H^+ \rightarrow H_2O_2 + OH^- \quad (5)$$

$$H_2O_2 + e^- \rightarrow OH^\bullet + OH^- \quad (6)$$

$$OH^\bullet + \text{organic matter (OM)} \rightarrow \text{degradation of OM} \quad (7)$$

$$h^+ + OM \rightarrow OM^{\bullet +} \rightarrow \text{oxidation of OM} \quad (8)$$

In this study, the photodegradation performance of rGO/ZnO/Cu in the aqueous solution of tetracycline under visible light was investigated. The response surface method (RSM) was employed to model and optimize the experimental condition for maximized TC degradation. Effect of initial pH, initial TC concentration, and rGO/ZnO/Cu concentration was studied. The total organic carbon (TOC) and removal percentage were determined to evaluate the mineralization. Kinetic study for specific conditions was implemented and rate constant (k) was calculated from curve fitting by pseudo-first and second-order model.

2. Experimental section

2.1. Reaction setup

Briefly, the photocatalytic degradation reaction was performed in a 500 mL batch reactor for 180 min. The light source was a 300 W Xe arc lamp (with ultraviolet cut off filter). A mixer with a pitched blade turbine mixed the suspension and an aquarium air pump injected air to the solution. The operating condition was adjusted to the desirable pH and temperature set to 25°C. The photocatalyst was prepared using a two-step ultrasonic-assisted method involving total reflux in the first step and hydrothermal process in the second step. The analyses used to characterize the photocatalyst are described with details elsewhere [25]. The rGO/ZnO/Cu concentration in photocatalytic suspension was 0.5, 1, 1.5, or 2 g/L. The pollutant suspension was prepared to use TC in four initial concentrations (40, 50, 60, or 70 mg/L). Finally, the two suspensions were combined to form the reaction suspension. Before irradiation, the mixture was stirred for 30 min to reach adsorption–desorption equilibrium. Initial pH was set to 6, 7, 8, or 9 using H_2SO_4 and NaOH solutions. At preselected periods 2 mL aliquots were taken and centrifuged several times to remove suspended pieces. All samples continued the chain reaction with hydroxyl radicals until they were quenched by adding H_2SO_4 (0.1 N) and kept them at 4°C for maximum of 2 d.

A sample of the solution was extracted at certain time intervals and examined through a UV-vis spectrophotometer after quenching and centrifugation. The maximum absorbance of TC was at wavelength 355 nm corresponding to the main characteristic peak. The TC concentration was calculated according to the Beer–Lambert's law from TC absorbency. The TC normalized temporal concentration is directly proportional to the normalized maximum absorbance (A_t/A_0 in 355 nm is equal to C_t/C_0).

2.2. Response surface method

In photocatalytic reactions, RSM has been used widely to minimize the number of experiments required to evaluate the effect of the operating parameters like pH, pollutant concentration, photocatalyst concentration, dissolved oxygen concentration, agitation speed, temperature, and irradiation time [25]. In this study, three influential independent parameters were evaluated: pH, rGO/ZnO/Cu concentration, and TC concentration. Toward this object, photocatalytic degradation of TC was optimized according to the five-level central composite design (CCD) method which is the most common form of RSM. Regression analysis was performed by Design-Expert® Software. The lower and upper limit values of variables are presented in Table 1. Table 2 shows the observed and predicted values of response for each run. The adequacy and significance of the model were judged based on analysis of variance (ANOVA) and coefficient of determination (R^2) which are summarized in Table 3.

Table 1
Experimental design ranges of independent variables

Coded variables	Factors	Levels				
		$-\alpha$	–1	0	1	$+\alpha$
A	pH	6	7	8	9	10
B	TC, mg/L	30	40	50	60	70
C	rGO/ZnO/Cu, g/L	0	0.5	1	1.5	2

Table 2
CCD design matrix for three variables with observed and predicted values for TC degradation

Run order	Coded value			Real values			Degradation efficiency (%)	
	A	*B*	*C*	*A*: pH	*B*: TC (mg/L)	*C*: rGO/ZnO/Cu(g/L)	Exp.	Pred.
1	0	0	2	8	50	2	80.01	80.04
2	0	0	0	8	50	1	94.37	93.97
3	0	0	0	8	50	1	95.11	93.97
4	1	1	–1	9	60	0.5	75.11	76.47
5	–1	–1	–1	7	40	0.5	83.34	83.31
6	0	2	0	8	70	1	85.64	86.87
7	0	0	0	8	50	1	94.95	93.97
8	–2	0	0	6	50	1	72.65	74.15
9	1	–1	–1	9	40	0.5	79.63	79.59
10	–1	1	1	7	60	1.5	83.16	83.13
11	1	–1	1	9	40	1.5	87.16	88.26
12	0	–2	0	8	30	1	99.35	100.34
13	0	0	–2	8	50	0	9.21	9.92
14	1	1	1	9	60	1.5	89.74	89.7
15	2	0	0	10	50	1	79.29	78
16	0	0	0	8	50	1	93.48	93.97
17	–1	–1	1	7	40	1.5	84.88	83.65
18	–1	1	–1	7	60	0.5	79.49	78.13

Table 3
ANOVA results for the response surface quadratic models

TC degradation	Source	Analysis of variance				
		Sum of squares	Df	Mean square	*F*-value	Prob > *F*
	Model	9.08×10^9	10	9.08×10^8	98.98	1.43×10^{-6}
	Residual	6.42×10^7	7	9.18×10^6		
	Lack of fit	5.48×10^7	4	1.37×10^7	4.36	0.13
	Pure error	9.43×10^6	3	3.14×10^6		

2.3. Measuring mineralization

TOC and TC removal were estimated through mineralization of the pollutant in a specified condition (pH: 8, TC concentration: 40 mg/L, rGO/ZnO/Cu: 1 g/L, irradiation time: 300 min).

3. Results and discussion

Below, we describe the effects of various operational conditions on TC degradation rate.

3.1. pH

pH is one of the major parameters impacting the photocatalytic degradation of organic pollutants, for example, tetracycline. Surface electrical properties of the photocatalyst, TC decomposition, and adsorption onto the rGO/ZnO/Cu and catalyst oxidation ability are important consequences of the pH changes [26,27]. The pH point of zero charge (pH_{PZC}) for rGO/ZnO/Cu was calculated 8.7 in this study. TC is an organic compound with an amphoteric molecule that is positively and negatively charged in acidic and alkaline conditions, respectively. The adsorption and dissociation constants (pKa) are influenced by the pH of the solution. At pH below 3.3, TC appears in the fully protonated form (H_3TC^+), is neutral (H_2TC) in the middle range of 3.3–7.68 and assumes anionic forms (HTC^- and TC^{2-}) in pH higher than 7.68. The pH_{PZC} of rGO/ZnO/Cu was specified at around 8.7. This means that either TC or photocatalyst, or both of them, will have a positive surface charge in acidic environment which increases repulsing electrostatic forces between the protonated forms of them. Therefore, degradation and removal efficiency decreased in acidic pH [28].

On the other hand, these repulsive forces appear again in basic pH higher than 8.7, because TC and rGO/ZnO/Cu nano photocatalyst will both be in anionic form. In a weak alkaline solution (7.68–8.7), electrostatic repulsion is substituted by attraction, because TC molecules change to the positive state and the photocatalyst has a negative

charge. Consequently, the highest adsorption could be seen in the range of weak basic near to neutral pH around 7.68–8.7. The other reason for increasing degradation rate refers to $OH^{\bullet}$ radicals which are a great help for TC hydrolysis. Under the alkaline condition, OH^- concentration increase on the rGO/ZnO/Cu surface creating more $OH^{\bullet}$ [29]. In the same way, positive holes have a significant role in oxidation. Under light irradiation, photo-excited charge converts O_2 to an active piece $O_2^{\bullet -}$, and holes are neutralized by OH^- ions to generate $OH^{\bullet}$. At the final step, TC is attacked by produced $OH^{\bullet}$ and $O_2^{\bullet}$ radicals, and photodegradation will be completed [30].

To understand the effect of initial pH, the aqueous suspension was made in the pH range of 6–9, adjusted by 1 M NaOH and H_2SO_4 solutions. As shown in Fig. 1, the removal efficiencies increased by increasing pH from 6 to 8 and have the maximum value (98.78%) in pH 8, but decrease after that with increasing the pH up to 9. A similar effect of pH was reported by Wang et al. [31] after 150 min [27].

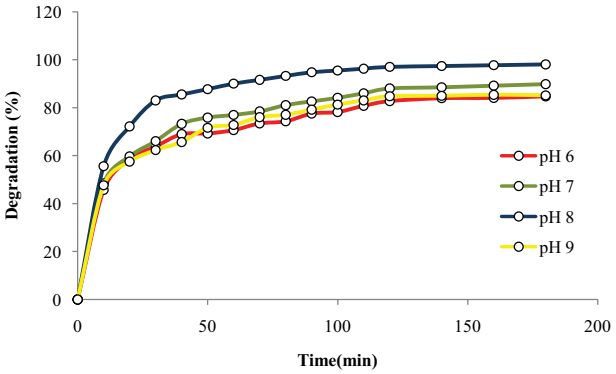

Fig. 1. Effect of pH on TC photodegradation (pH: 6, 7, 8, and 9, TC concentration: 40 mg/L, and rGO/ZnO/Cu concentration: 1 g/L).

3.2. rGO/ZnO/Cu concentration

Fig. 2 shows the removal of TC at different concentrations of rGO/ZnO/Cu. TC degradation under visible light was very slow without a photocatalyst. When the ZnO complex concentration was increased up to 1 g/L, the reaction rate went up presumably because more adsorption sites were produced and more $OH^{\bullet}$ radicals became available for photoreactions. The optimal concentration of the ZnO complex for removal of 40 mg/L TC at pH = 8 was 1 g/L. Further increasing the photocatalyst concentration was detrimental and retarded the reaction. We believe that this happened for two reasons: firstly, agglomeration and sedimentation of the catalyst effectively eliminated a high fraction of active sites from the reaction environment; secondly, the abundance of suspended particles in the solution blocked the penetration of visible light or misled it to the wrong direction [32]. This is consistent with previous reports [26,31].

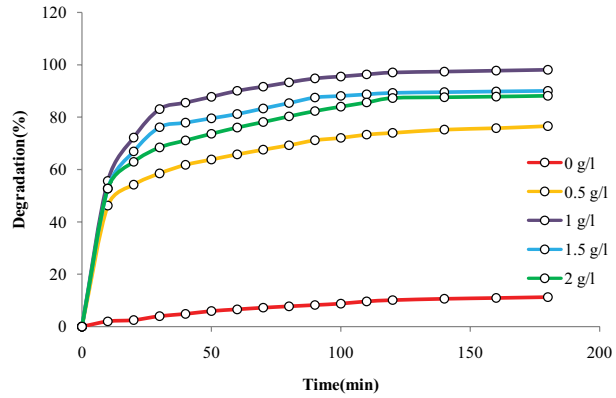

Fig. 2. Effect of the photocatalyst concentration on TC photodegradation (pH: 8, TC concentration: 40 mg/L, and rGO/ZnO/Cu concentration: 0, 0.5, 1, 1.5, and 2 g/L).

3.3. TC initial concentration

Fig. 3 shows TC degradation rates starting from concentrations 40, 50, 60, or 70 mg/L, for 180 min under visible light irradiation. The experimental data display lower removal rates at higher TC concentrations. This could be because of one of the following reasons. In lower TC concentration, the kinetic regime controls the progress of the reaction, but when it goes higher, the mass transfer becomes the limiting factor [26]. By increasing pollutant concentration, more product is produced during irradiation, $OH^{\bullet}$ radicals are captured between them and become the limiting reactant, thus diminishing the degradation rate [33]. Under these circumstances, a high concentration of TC molecules accumulates on the photocatalyst surface effectively inhibiting the subversion mechanism. Increased turbidity in the suspension further impedes TC molecules from contact with the photogenerated holes and hydroxyl radicals [34]. The amount of generated hydroxyl radicals remains constant against increasing TC concentration which leads to lower

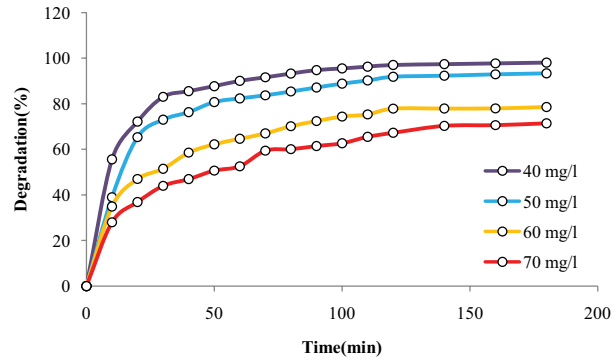

Fig. 3. Effect of initial TC concentration on the photodegradation (pH: 8, TC concentration: 40, 50, 60, and 70 mg/L, and rGO/ZnO/Cu concentration: 1 g/L).

availability of reactant radicals per TC molecule and diminishing degradation efficiency.

After exploring the effect of individual factors on TC removal rates, we integrated them into a unified regression model to obtain the optimal set of conditions for TC degradation using the RSM.

3.4. Regression model equation and optimization of TC degradation using RSM

The removal percentages of TC in the actual and predicted form are presented in Table 2. The photodegradation efficiency varied from 11.21% for photolysis to 98.78% for pH = 8, 1 g/L rGO/ZnO/Cu, and 40 mg/L TC. The relationship between the response and operating variables was modeled with a polynomial reduced cubic equation after elimination of insignificant terms (p-value > 0.05):

$$(\text{Degradation})^{2.51} = 89{,}573.61 + 1{,}671.79 \times A - 8{,}013.01 \times B + 14{,}890.77 \times C + 1{,}057.91 \times AB + 4{,}202.48 \times AC + 2{,}205.27 \times BC - 9{,}197.85 \times A^2 - 14{,}866.82 \times C^2 + 6{,}347.35 \times A^2B - 8{,}144.066 \times A^2C \quad (9)$$

where A is pH, B is TC concentration (mg/L), and C is photocatalyst concentration (g/L). The ANOVA is presented in Table 3. Statistical significance is indicated by a low probability value (p-value < 0.0001). The coefficient of determination (R^2) which measures the goodness-of-fit of the model was 0.9930. The adjusted R^2 was 0.9829 which is in a good agreement with the predicted correlation coefficient squared (pred. R^2), 0.9343. High accordance with adj. R^2 and pred. R^2 confirms that the empirical model has captured the significant factors impacting the response well.

The maximum value of TC degradation based on the optimization results of RSM is obtained with a predicted yield as high as 91.55%. The coded and real variables associated with the maximum objective function value are reported in Table 4.

3.5. Importance of variables and interactions on TC degradation

The derived model equation shows some properties of the system's behavior. The baseline degradation efficiency could be calculated from the intercept of the model. In this case, the response variable is modified by the power transformation (2.51), and therefore, the baseline degradation rate (where all independent variables are set to 0) is determined by 2.51th root of the intercept. This parameter in Eq. (9) calculated 93.96% ($89{,}573.61^{1/2.51} = 93.96$). Although there would be no degradation if initial TC concentration were exactly zero, this value indicates the likely degradation rate if very small initial TC and catalyst concentrations had been tested in an extremely acidic environment. More interestingly, the sign and magnitude of each coefficient represent how much and in which direction they affect TC degradation. Coefficients of interaction terms demonstrate synergistic (+) and antagonistic (–) effects [29]. Accordingly, rGO/ZnO/Cu concentration (C) is the most influential and other terms followed by TC concentration (B) and initial pH (A).

Figs. 4–6 depict interaction patterns of pairs of independent variables via contour plots and surface response plots. The interactive effect of the TC concentration and photocatalyst concentration is presented in Fig. 5. It indicates that the degradation rate increased with increasing TC or rGO/ZnO/Cu concentration up to their optimum mass ranges, then it goes down by increasing the concentration of each factor. This observation has some reasons, like enhancing the number of reaction sites on the surface of the photocatalyst. The expanded active surface area adds to the number of radicals attacking the pollutant molecules and improves degradation efficiency. Although a relatively high concentration of photocatalyst increases pollutant degradation, the excess amount of it will cause solution turbidity and blocks light penetration which harms the photodegradation percentage. Besides, a very high rGO/ZnO/Cu concentration results in the agglomeration of particles and a reduced number of available sites for light absorption on the photocatalyst surface [29]. The maximum degradation occurred in the maximum rGO/ZnO/Cu and minimum TC concentrations; more TC needs higher photocatalyst concentration to hold degradation performance at a constant level.

Fig. 4 shows the response surface and contour plot of the photocatalytic degradation rate of TC vs. pH of the solution and rGO/ZnO/Cu concentration. As mentioned in section 3.1 (pH), the pH point of zero charge for the rGO/ZnO/Cu complex is around 8.7 [25]. The reaction rate is low in low pH and small photocatalyst concentrations. Raising pH and photocatalyst concentration increases the degradation rate up to 98.78%. Beyond that peak, reaction rate declines again due to the saturation of adsorption capacity, changes in visible light penetration and the behavior of charged groups and free radicals.

The effect of pH and TC concentration is shown in Figs. 6a and b. The removal efficiency decreases when pH deviates from the optimum value of 8, and from the minimum TC content, due to the repulsion force described before in section 3.1 (pH) [28]. It is completely in line with the effect of each of these operating parameters. According to the literature, Mazarji et al. [29] and Arsalani et al. [30] reported the same result for other pollutants. They also demonstrated their claims with RSM plots and a final equation model.

Table 4
Optimum values of the operating conditions in TC degradation, and experimental and predicted values on optimal conditions

Parameter	Optimum value
pH	8.8905
TC	59.7874
rGO/ZnO/Cu	0.8302
TC degradation (%) Pred.	91.55
TC degradation (%) Exp.	87.64

3.6. Recycled photocatalytic activity of rGO/ZnO/Cu

Fig. 7 shows recycling runs of the rGO/ZnO/Cu for the photodegradation of TC in optimal operating conditions. The recycle experiments were done to evaluate the stability of rGO/ZnO/Cu with three consecutive cycles at the optimal operating conditions. In the recycling experiments, the photocatalyst was separated from the reaction system by simple filtering first, then it was centrifuged and washed several times before drying in the oven. After recovering the photocatalyst, a fresh solution of the pollutant was prepared for the next run to evaluate the photocatalytic

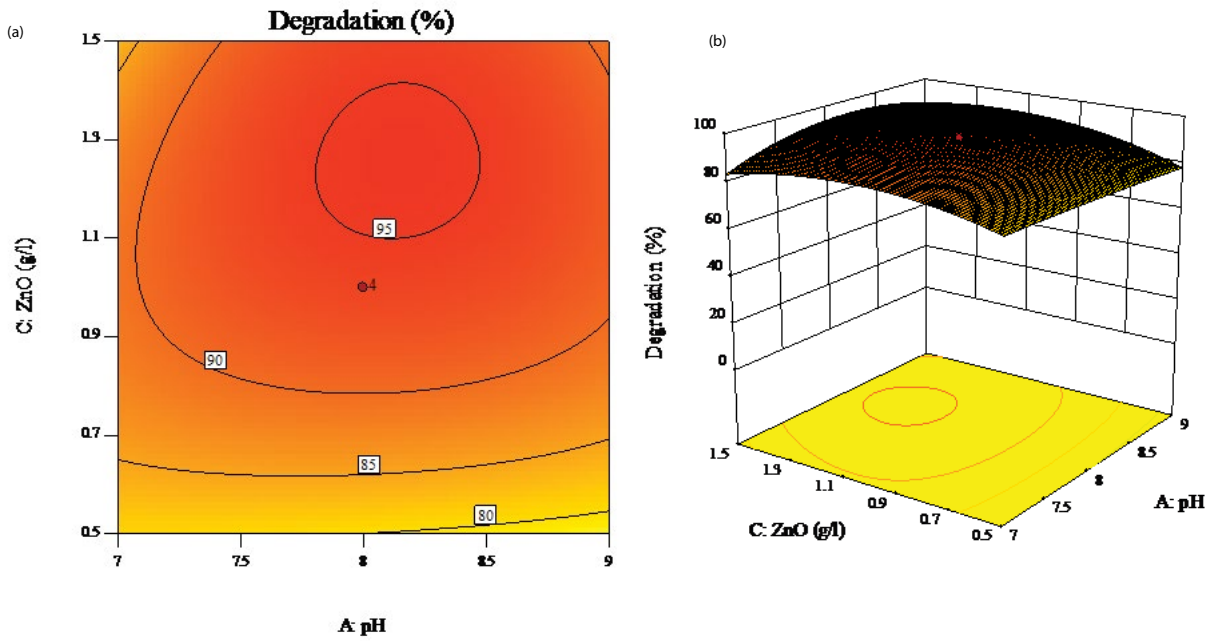

Fig. 4. (a) Contour plot and (b) response surface of TC degradation as a function of pH and photocatalyst concentration.

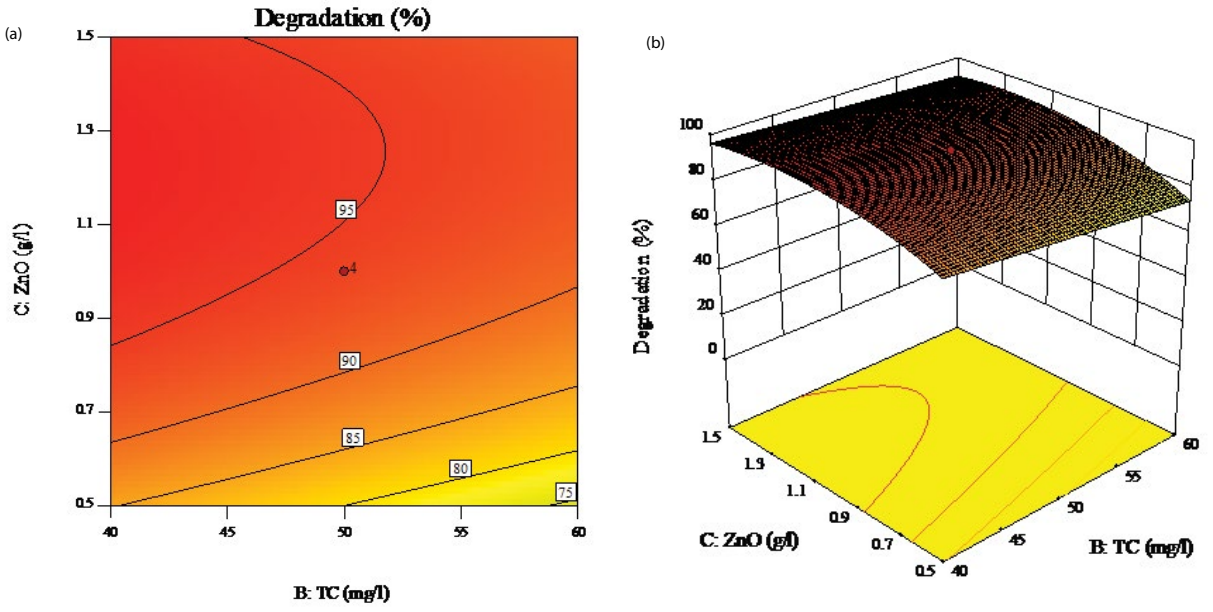

Fig. 5. (a) Contour plot and (b) response surface of TC degradation as a function of TC concentration and photocatalyst concentration.

ability of the recovered photocatalyst. These steps were repeated two times under the same conditions. Results are presented in Fig. 7. As can be observed, the photocatalytic degradation efficiency decreased only slightly, from 88.98% to 84.24%, which confirms that the photocatalyst is stable and reusable under these conditions.

3.7. Kinetic study of TC degradation

The kinetic analysis for photocatalytic degradation of TC was conducted to explore the mechanism of pollutant degradation. The pseudo-first-order kinetic model was used in linear form as according to the following equation:

$$\ln\frac{C_t}{C_0} = k_1 t \tag{10}$$

where C_t is the TC concentration at time t (mg/L), C_0 is the initial TC concentration (mg/L), k_1 is the observed rate constant (1/min), and t is time (min). k_1 could be estimated from the slope of a straight line regressing $\ln(C_t/C_0)$ vs. t.

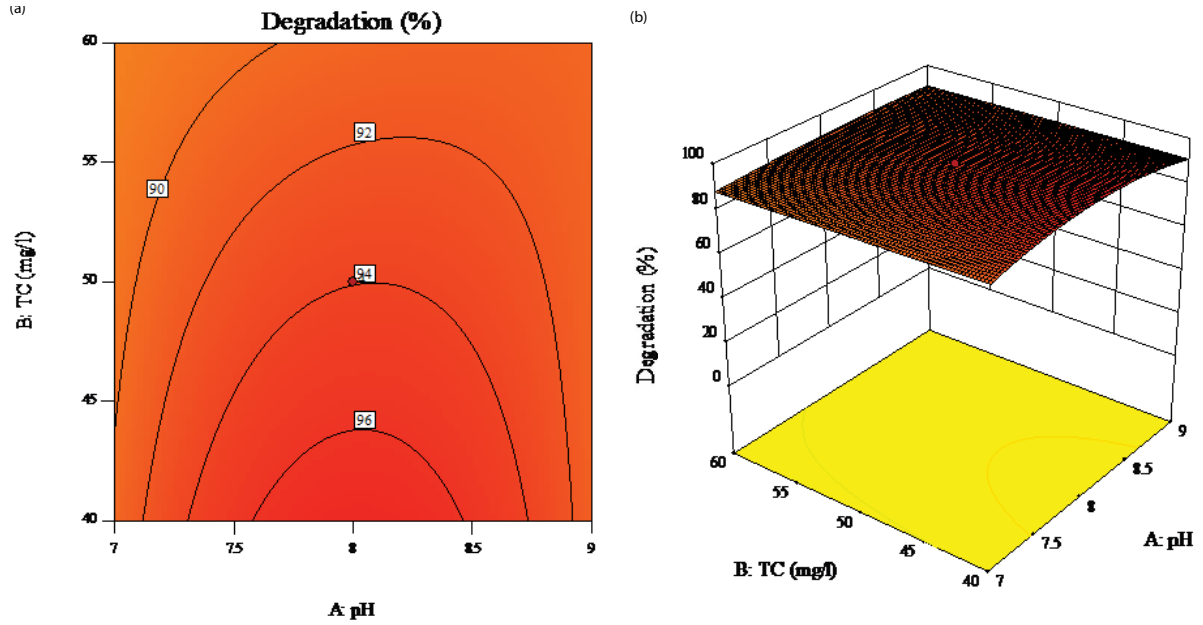

Fig. 6. (a) Contour plot and (b) response surface of TC degradation as a function of pH and TC concentration.

The higher regression coefficients are desirable to reach the best-fitted model on experimental data presented in Table 5. Similarly, the rate constant in a pseudo-second-order can be calculated as the slope of the 1/*C* vs. *t* regression line (Eq. (11)):

$$\frac{1}{C_t}-\frac{1}{C_0}=k_2 t \tag{11}$$

where C_t is the TC concentration at time t (mg/L), C_0 is the initial TC concentration (mg/L), k_2 is the observed rate constant (L/min/mg) and t is time (min). Table 5 shows the goodness-of-fit measure, R^2, for these two models fitted to our experimental data. The pseudo-second-order model fit the data better under all experimental conditions with $R^2 > 0.9$. Therefore, the rate constant is reported only for this model. According to the obtained data, degradation rate constant (k_2) increased with an increase in pH from 6 to 8 from 0.00075 to 0.00727 L/min/mg, then by enhancing pH up to 9, k_2 has a significant drop to 0.00085 L/min/mg. Mazarji et al. [29] found similar results. The degradation rate constant was very small for 0.5 g/L photocatalyst, but there was an increase in k_2 from 0.5 to 1.5 g/L, and the rate constant goes from 0.000401 to 0.001308 L/min/mg. These calculations confirm our conclusions from exploring the corresponding plots discussed above (Figs. 1 and 2). Safari et al. [26] degraded TC using TiO_2 and found kinetic rate constant obtained from the pseudo-first model increase by pH increasing. They also found increasing photocatalyst concentration enhanced kinetic rate constant up to an optimum point and then led to diminishing k_1 consistent with the results of this study [26].

Also, as Table 5 shows, higher TC concentration hurts the k_2 values in this study, which is explained by two reasons: (1) By increasing pollutant concentration, more active sites

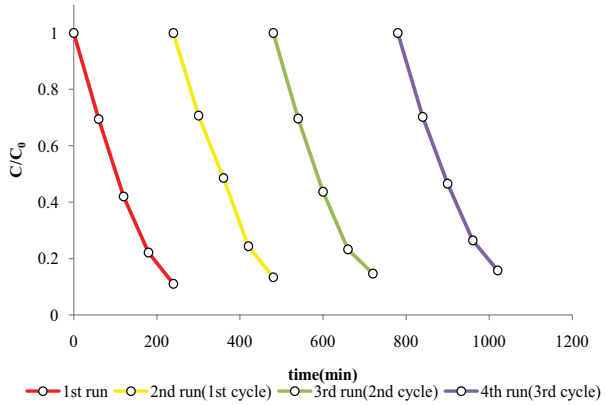

Fig. 7. Reusability of the rGO/ZnO/Cu in optimal operating conditions (pH: 9, TC concentration: 60 mg/L, and rGO/ZnO/Cu: 1 g/L).

are coated and thus the generation of $OH^{\bullet}$ radicals becomes harder. (2) The other factor is decreasing the path length of a photon entering the suspension due to turbidity, and thus decreasing degradation efficiency [29]. It's also reported in the research of Ahmadi et al. [5] that degradation rate constant (k_1) decreased from 0.0642 to 0.0316 1/min when TC concentration increased from 10 to 30 mg/L. Kakavandi et al. [32] fitted their experimental data with zero, first, and second-order models and found TC concentration influenced the degree of the fitted model [32].

The value of tetracycline TOC removal was quantified during 300 min (1 g/L rGO/ZnO/Cu; pH: 8; TC concentration: 40 mg/L) and shown in Fig. 8. Approximately, 82% and 100% of TOC and TC were removed after 180 min irradiation, respectively. In the following 120 min, the mineralization and TC removal rate plateaued and reached near completion

Table 5
Kinetic modeling under different operating conditions (pH, photocatalyst concentration, and TC concentration)

Operating parameter		R^2		
		k_2 (L/min/mg)	First-order-kinetic	Second-order-kinetic
TC concentration: 40 mg/L, rGO/ZnO/Cu: 1 g/L	pH 6	0.00075	0.831	0.964
	pH 7	0.00126	0.863	0.983
	pH 8	0.00727	0.906	0.962
	pH 9	0.00085	0.831	0.948
		rGO/ZnO/Cu concentration		
pH: 8, TC concentration: 40 mg/L	0	0.000018	0.927	0.934
	0.5 g/L	0.000401	0.744	0.905
	1 g/L	0.007280	0.906	0.962
	1.5 g/L	0.001308	0.758	0.929
	2 g/L	0.001075	0.831	0.961
		TC concentration		
pH: 8, rGO/ZnO/Cu: 1 g/L	40 mg/L	0.00727	0.906	0.962
	50 mg/L	0.00204	0.868	0.985
	60 mg/L	0.00052	0.838	0.938
	70 mg/L	0.00031	0.887	0.967

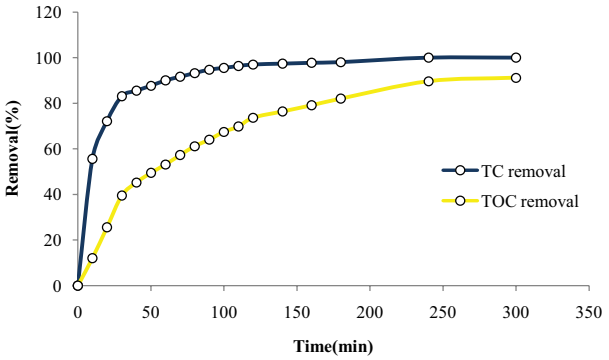

Fig. 8. Mineralization of TC in the form of TC and TOC removal (pH: 8, TC concentration: 40 mg/L, and rGO/ZnO/Cu: 1 g/L).

at the end. In previous studies, the stagnation of the mineralization plot is reported, which indicated the formation of long-lived by-products [35].

4. Conclusion

Photocatalytic degradation of tetracycline in aqueous solutions was investigated under visible light using a synthetic rGO/ZnO/Cu compound as photocatalyst. The highest photocatalytic degradation of TC was achieved at pH = 8, TC = 40 mg/L, and rGO/ZnO/Cu = 1 g/L. Kinetic study on the operating conditions showed good agreement with a pseudo-second-order model, with $R^2 > 0.9$ in all cases. The degradation rate constant decreased with increasing TC concentration. By increasing the photocatalyst concentration and pH, the TC removal rate picked up at first and then declined after the points of optimum. TOC and TC removal was achieved by 82% and 100% after 300 min.

References

[1] R.D.P. Drogui, Tetracycline antibiotics in the environment: a review, Environ. Chem. Lett., 11 (2013) 209–227.
[2] C. Yuan, C. Hung, H. Li, W. Chang, Photodegradation of ibuprofen by TiO_2 co-doping with urea and functionalized CNT irradiated with visible light–effect of doping content and pH, Chemosphere, 155 (2016) 471–478.
[3] Y. Fu, L. Peng, Q. Zeng, Y. Yang, H. Song, J. Shao, S. Liu, J. Gu, High efficient removal of tetracycline from solution by degradation and flocculation with nanoscale zerovalent iron, Chem. Eng. J., 270 (2015) 631–640.
[4] X. Jing, Y. Wang, W. Liu, Y. Wang, H. Jiang, Enhanced adsorption performance of tetracycline in aqueous solutions by methanol-modified biochar, Chem. Eng. J., 248 (2014) 168–174.
[5] M. Ahmadi, H. Ramezani, N. Jaafarzadeh, Enhanced photocatalytic degradation of tetracycline and real pharmaceutical wastewater using MWCNT/TiO_2 nano-composite, J. Environ. Manage., 186 (2017) 55–63.
[6] M.H. Khan, H. Bae, J. Jung, Tetracycline degradation by ozonation in the aqueous phase: proposed degradation intermediates and pathway, J. Hazard. Mater., 181 (2010) 659–665.
[7] G.M. Bistan, The relevance of bisphenol A adsorption during Fenton's oxidation, Int. J. Environ. Sci. Technol., 10 (2013) 1141–1148.
[8] H. Liu, Y. Yang, J. Kang, M. Fan, J. Qu, Removal of tetracycline from water by Fe-Mn binary oxide, J. Environ. Sci., 24 (2012) 242–247.
[9] A. Mahvi, Application of ultrasonic technology for water and wastewater treatment, Iran. J. Public Health, 38 (2009) 1–17.
[10] A.O. Ifelebuegu, J.O.E. Joyce, T. Mason, Sonochemical degradation of endocrine disrupting chemicals 17b-estradiol and 17a-ethinylestradiol in water and wastewater, Int. J. Environ. Sci. Technol., 11 (2014) 1–8.
[11] L. Wang, Photosonochemical degradation of phenol in water, Water Res., 35 (2001) 3927–3933.
[12] N. Dobaradran, S. Nabizadeh, R. Mahvi, A.H. Mesdaghinia, A.R. Naddafi, K. Yunesian, M. Rastkari, Survey on degradation rates of trichloroethylene in aqueous solutions by ultrasound, Iran. J. Environ. Health Sci. Eng., 7 (2010) 307–312.

[13] K.M. Lee, C.W. Lai, K.S. Ngai, J.C. Juan, Recent developments of zinc oxide based photocatalyst in water treatment technology: a review, Water Res., 88 (2016) 428–448.
[14] A. Janotti, C.G. Van de Walle, Fundamentals of zinc oxide as a semiconductor, Rep. Prog. Phys., 72 (2009) 126501.
[15] A.K. Das, P. Misra, R.S. Ajimsha, V.K. Sahu, B. Singh, Electron interference effects and strong localization in Cu doped ZnO thin films, Mater. Sci. Semicond. Process., 68 (2017) 275–278.
[16] G. Torres-Hernández, J.R. Ramírez-Morales, E. Rojas-Blanco, L. Pantoja-Enriquez, J. Oskam, G. Paraguay-Delgado, F. Escobar-Morales, B. Acosta-Alejandro, M. Díaz-Flores, L.L. Pérez-Hernández, Structural, optical and photocatalytic properties of ZnO nanoparticles modified with Cu, Mater. Sci. Semicond. Process., 37 (2015) 87–92.
[17] L.K. Putri, W.-J. Ong, W.S. Chang, S.-P. Chai, Heteroatom doped graphene in photocatalysis: a review, Appl. Surf. Sci., 358 (2015) 2–14.
[18] F. Guinea, M.I. Katsnelson, A.K. Geim, Energy gaps and a zero-field quantum Hall effect in graphene by strain engineering, Nat. Phys., 6 (2010) 30–33.
[19] W. Kang, X. Jimeng, W. Xitao, The effects of ZnO morphology on photocatalytic efficiency of ZnO/RGO nanocomposites, Appl. Surf. Sci., 360 (2016) 270–275.
[20] H.R. Pant, C.H. Park, P. Pokharel, L.D. Tijing, D.S. Lee, C.S. Kim, ZnO micro-flowers assembled on reduced graphene sheets with high photocatalytic activity for removal of pollutants, Powder Technol., 235 (2013) 853–858.
[21] K. Ravichandran, N. Chidhambaram, S. Gobalakrishnan, Copper and graphene activated ZnO nanopowders for enhanced photocatalytic and antibacterial activities, J. Phys. Chem. Solids, 93 (2016) 82–90.
[22] D. Kanakaraju, B.D. Glass, M. Oelgemo, Titanium dioxide photocatalysis for pharmaceutical wastewater treatment, Environ. Chem. Lett., 12 (2014) 27–47.
[23] X. Zhu, Y. Wang, R. Sun, D. Zhou, Photocatalytic degradation of tetracycline in aqueous solution by nanosized TiO_2, Chemosphere, 92 (2013) 925–932.
[24] L. Yang, L.E. Yu, M.B. Ray, Degradation of paracetamol in aqueous solutions by TiO_2 photocatalysis, Water Res., 42 (2008) 3480–3488.
[25] A. Mondaca, A. Giraldo, G. Pen, R.A. Palominos, D. Mansilla, Photocatalytic oxidation of the antibiotic tetracycline on TiO_2 and ZnO suspensions, Catal. Today, 144 (2009) 100–105.
[26] G.H. Safari, M. Hoseini, M. Seyedsalehi, H. Kamani, J. Jaafari, A.H. Mahvi, Photocatalytic degradation of tetracycline using nanosized titanium dioxide in aqueous solution, Int. J. Environ. Sci. Technol., 12 (2015) 603–616.
[27] F. Saadati, N. Keramati, M.M. Ghazi, Influence of parameters on the photocatalytic degradation of tetracycline in wastewater: a review, Crit. Rev. Env. Sci. Technol., 46 (2016) 757–782.
[28] A. Mirzaei, L. Yerushalmi, Z. Chen, F. Haghighat, Photocatalytic degradation of sulfamethoxazole by hierarchical magnetic ZnO@g-C_3N_4: RSM optimization, kinetic study, reaction pathway and toxicity evaluation, J. Hazard. Mater., 359 (2018) 516–526.
[29] M. Mazarji, G. Nabi-bidhendi, N. Mohammad, One-pot synthesis of a reduced graphene oxide – ZnO nanorod composite and dye decolorization modeling, J. Taiwan Inst. Chem. Eng., 80 (2017) 439–451.
[30] N. Arsalani, R. Nasiri, M. Zarei, Synthesis of magnetic 3D graphene decorated with $CaCO_3$ for anionic azo dye removal from aqueous solution: kinetic and RSM modeling approach, Chem. Eng. Res. Des., 136 (2018) 795–805.
[31] H. Wang, H. Yao, J. Pei, F. Liu, D. Li, Photodegradation of tetracycline antibiotics in aqueous solution by UV/ZnO, Desal. Water Treat., 57 (2016) 19981–19987.
[32] B. Kakavandi, A. Takdastan, N. Jaafarzadeh, M. Azizi, A. Mirzaei, A. Azari, Application of Fe_3O_4@C catalyzing heterogeneous UV-Fenton system for tetracycline removal with a focus on optimization by a response surface method, J. Photochem. Photobiol., A, 314 (2016) 178–188.
[33] D. Dimitrakopoulou, I. Rethemiotaki, Z. Frontistis, N.P. Xekoukoulotakis, D. Venieri, D. Mantzavinos, Degradation, mineralization and antibiotic inactivation of amoxicillin by UV-A/TiO_2 photocatalysis, J. Environ. Manage., 98 (2012) 168–174.
[34] R. Mohammadi, B. Massoumi, M. Rabani, Photocatalytic decomposition of amoxicillin trihydrate antibiotic in aqueous solutions under UV irradiation using Sn/TiO_2 nanoparticles, Int. J. Photoenergy, 2012 (2012) 1–11.
[35] W. Cun, Z. Jincai, W. Xinming, M. Bixian, Preparation, characterization and photocatalytic activity of nano-sized ZnO/SnO_2 coupled photocatalysts, Appl. Catal., B, 39 (2002) 269–279.